Final Report for the OZONE SAF

Visiting Scientist Grant (P-5779-12-03)

October 05, 2004

Development of the Linearized Vector Radiative Transfer Model VLIDORT

Robert J. D. Spurr[1], Jukka Kujanpaa[2]

[1] *Harvard-Smithsonian Center for Astrophysics,*
60 Garden Street, Cambridge, MA 02138, USA
Email: rspurr@cfa.harvard.edu

[2] *Ozone and UV Radiation Research, Finnish Meteorological Institute,*
Vuorikatu 19, P.O.BOX 503, FIN-00101 Helsinki, Finland
Email: Jukka.Kujanpaa@fmi.fi

1 Overview

This Final report covers the 8-month period from the beginning of February 2004 to beginning of October 2004, and summarizes GOME-2 research activities conducted by O_3 SAF Visiting Scientist (VS) Dr. Robert Spurr of the Harvard-Smithsonian Center for Astrophysics in connection with the development of a vectorized version of LIDORT.

In the mid-term review (July 2004), it was reported that the main VLIDORT development has been completed, with the multiple-scattering vector LIDORT model in the pseudo-spherical approximation. Initial benchmark validations were reported.

In this final report, we concentrate on new developments which include (a) additional validation against benchmark Rayleigh atmosphere results (b) first results for a realistic 22-layer Rayleigh atmosphere with ozone absorption, and (c) initial results including aerosols in the multi-layer application. A User's Guide has been written to accompany this final report.

We summarize the background and motivation (next section), then review the main aspects of the model in Section 3, describe all benchmark validation tests in Section 4 and summarize new results in Section 5. Concluding remarks in Section 6 point to further work required for the completion of VLIDORT.

2 Background and Motivation

Studies with GOME have shown that the treatment of polarization is critical for the successful retrieval of ozone profiles. In particular: (1) the polarization correction to Level 1b data derived only from PMD measurements has proved to be insufficiently accurate, and has required a better description using vector RT modeling; and (2) forward modeling of radiances should be done using a vector treatment including polarization, as the use of a scalar model can lead to considerable errors for some scenarios. Similar considerations apply to radiance-based surface UV algorithms. Both these algorithms require measurements over the UV spectrum between 300-325 nm, for which the wide variation in polarization behavior is critical.

For ozone profiling, a work-around solution has been developed for the inclusion of polarization in the forward modeling. A large look-up table of polarization corrections has been generated off-line using a vector model, and this table is designed to provide corrections for the on-line computation of radiances (weighting functions are not corrected). This is in some ways a stop-gap solution (it combines output from two very different RT models). Ideally we require a single dedicated vector radiative transfer model that will not only compute backscattered radiation with full polarization, but also (with the linearization capacity for weighting function generation) find use directly in an advanced retrieval algorithm ingesting GOME-2 measurements in two planes of polarization. GOME-2 has a more sophisticated capacity for measuring polarized light then GOME-1, and the use of a vector model is more critical.

The forward scalar (non-polarized) RT model LIDORT [1-5] developed by R. Spurr at CfA in the past four years is in widespread use now for the major GOME-2 algorithms. The UV Product algorithm developed at FMI uses LIDORT for calculations of backscatter radiances. The ozone profile algorithm at KNMI uses a modified fast 6-stream model called LIDORTA for the generation of radiances and weighting functions, while the total ozone column algorithm at DLR is also using LIDORT (in the latest V2PLUS incarnation) for the calculations of Air Mass Factors. The model has a full multiple-scatter treatment (essential in the UV and visible) for a multi-layer atmosphere. Version 2.3 of LIDORT has the pseudo-spherical approximation for the attenuation of the solar beam in a curved shell atmosphere, and Version V2PLUS (2003) has a dedicated sphericity correction to deal with simulations involving wide viewing angles at the GOME-2 swath ends. Version 2.4 deals with non-Lambertian surfaces. There is also a version with first-order inelastic rotational Raman scattering (LIDORT-RRS, developed in 2002 as part of the O3SAF VS program).

The development of a vectorized version of LIDORT is of major importance in its own right, quite aside from the logical extensions it offers to existing LIDORT models currently in use at SAF institutes. It is anticipated that the generic nature of the discrete ordinate vector RT model formalism will ensure that VLIDORT will find many uses in passive remote sensing. We can now report that the VLIDORT model has been completed and tested, and in the next two sections we summarize these aspects.

3 VLIDORT Model Summary

Although the Stokes vector formalism for radiative transfer was worked out by Chandrasekhar in the 1940s [6], it was only in the 1980s that the mathematics of the vector RT equations was fully explored, in particular with the papers of Siewert and co-workers [7-11], and also work done by the Dutch group under Hovenier [12-15]. In 1998, Siewert [16-17] revisited the discrete ordinate slab problem in plane-parallel geometry, and his penetrating analysis revealed that the presence of complex variable solutions to the vector equations is an essential part of the problem. Siewert was able to provide benchmark results which agree perfectly with results obtained earlier using other solution methods (spherical harmonics [10], the F-N method [11], and doubling-adding [18]).

In VLIDORT we follow Siewert's formalism regarding the solution of the homogeneous equations of vector radiative transfer. As with the scalar case, there is a Fourier series decomposition in the cosine of the relative azimuth, for the Stokes vector and the scattering phase matrix. If there are 4 Stokes components and N streams in the half-space, the reduction of order method yields a $4N$x$4N$ eigenproblem which is solved using the LAPACK package DGEEV. Real eigenvalues occur in pairs $\pm k_\alpha$; complex eigenvalues in conjugate pairs. The RT solution is then written as linear combinations of the real eigenvectors and the real part of the complex eigenvectors, the resulting linear coefficients (integration constants) to be determined through imposition of the boundary conditions.

For the solar beam source term, Siewert [17] used a Green's function method which expresses the particular solution in terms of combinations of the eigensolutions. This technique is an alternative to the more traditional linear-algebra method which relies on a substitution of the form $\mathbf{I} \sim \mathbf{Q}\exp(-\lambda x)$ for optical thickness x and average secant λ in the pseudo-spherical formulation. The scalar LIDORT models from Version 2.1 onwards have both implementations. Here we have chosen not to use the Green's function method for a very simple reason - the algebraic bookkeeping is much more extensive. Instead, we implemented the linear-algebra technique (again with a reduction in order to a $4N$x$4N$ problem). This is a new solution for the vector model, and the fact that we were able to reproduce exactly Siewert's results for the slab indicates the robustness of our model.

The boundary value problem $\mathbf{A}.\mathbf{X} = \mathbf{B}$ is set up and solved in the usual way for a multi-layer atmosphere. The slab problem requires only the top of atmosphere condition (no diffuse radiance downwelling) and the surface reflectance condition. We introduced continuity conditions for intermediate layer boundaries. LAPACK routines DGETRF (SVD decomposition) and DGETRS (back-substitution) were used for the slab problem (one layer), while routines DGBTRF and DGBTRS (SVD with band compression) were used for multi-layer solutions. An important point to make here is that the multi-layer capability can easily be tested using Ambartsumian's invariance principle - two optically identical layers of optical thicknesses x_1 and x_2 will (at least for plane-parallel geometry) produce a field equivalent to that produced by an optically identical layer of thickness $x_1 + x_2$.

VLIDORT is organized in the same fashion as the LIDORT code. Post processing follows the source function integration technique; this is a smart interpolation to generate output at polar directions away from the discrete ordinate streams. Set-ups for transmittance factors and the construction of pseudo-spherical parameterizations of the solar beam attenuation are similar to those in the scalar model. The derivation of Legendre polynomials for the scattering matrix is much more complicated, and like many other workers in the field, we follow the formalism of Siewert [8]. At the time of writing the surface reflectance condition is confined to Lambertian reflectance (which is not polarizing), but the BRDF formalism that was coded up for the scalar LIDORT Version 2.4 has been incorporated in VLIDORT and awaits suitable inputs for testing.

Inputs to VLIDORT are (1) layer total single scatter albedos; (2) layer optical thickness values; and (3) layer "Greek matrices" of scattering properties. Inputs (1) and (2) are the same as for the scalar code. The 4x4 matrix input (3) is based on six "Greek constants" $\{\alpha_l, \beta_l, \gamma_l, \eta_l, \epsilon_l and \delta_l\}$

which must be specified for each moment l of a Legendre function expansion in terms of the cosine of the scattering angle. The values β_l are the usual phase function moments, the ones that appear as inputs to the scalar version.

One very important feature that was implemented at the outset is the capability to handle multiple solar zenith angles simultaneously. This feature is not present in any of the scalar LIDORT codes in F77, but it was implemented late in 2003 as part of the first LIDORT F90 model. By introducing an internal loop over solar zenith angles inside the model, one can find homogeneous solutions and the inverse boundary value matrix $\mathbf{A}^{-1}$ before this solar beam loop. These time-consuming tasks need only to be done once, and it is then a matter for repeated determinations of the particular integrals for various solar beam forcings, followed by boundary value back-substitutions and post-processing. This is a very substantial performance enhancement for VLIDORT, particularly in view of the increased time taken over the eigenproblem (complex roots) and the much larger BVP matrix inversion.

In summary, the capabilities are:
- pseudo-spherical solar beam attenuation;
- linear-algebra solution of particular integrals;
- arbitrary viewing geometry and optical depth output;
- downwelling and/or upwelling output;
- flux/mean-intensity output options;
- multiple scatter layer source term output;
- multi-solar beam output;
- complete scalar output as validation.

The code was written in Fortran 77. Version 1.0 of the code will be released as a package complete with User's Guide. The developmental version used double precision floating point as the baseline, and Complex*16 variables to deal with the complex eigenproblem values. In the release version 1.0, complex variables have been replaced by pairs of double precision variables, partly to avoid compilation problems and partly to avoid redundancy. The code is now fully portable and has been tested on three independent platforms.

4 Benchmark Validation

VLIDORT is designed to work equally with Stokes 4-vectors $\{I,Q,U,V\}$ or 3-vectors $\{I,Q,U\}$, and of course in the scalar mode (I only). The first task for the vector model is to run it with only one Stokes component (the total intensity) and reproduce results generated independently from the scalar LIDORT model. A set of options can be used to test the major functions of the model (the *real* RT solutions, the boundary value problem and post processing) for the usual range of scenarios (single layer, multilayer, arbitrary optical thickness and viewing angles, plane-parallel

Op.depth–>	0.000	0.125	0.250	0.500	0.750	0.875	1.000
-1.00000	5.06872E-02	4.26588E-02	3.45652E-02	1.97273E-02	7.87441E-03	3.36768E-03	
-0.90000	4.49363E-02	3.83950E-02	3.16314E-02	1.87386E-02	7.81148E-03	3.42290E-03	
-0.80000	4.95588E-02	4.29605E-02	3.59226E-02	2.19649E-02	9.46817E-03	4.21487E-03	
-0.70000	5.54913E-02	4.89255E-02	4.16034E-02	2.63509E-02	1.18019E-02	5.35783E-03	
-0.60000	6.19201E-02	5.57090E-02	4.83057E-02	3.18640E-02	1.49296E-02	6.94694E-03	
-0.50000	6.84108E-02	6.30656E-02	5.59610E-02	3.87231E-02	1.91563E-02	9.19468E-03	
-0.40000	7.44303E-02	7.06903E-02	6.44950E-02	4.72940E-02	2.50375E-02	1.25100E-02	
-0.30000	7.89823E-02	7.78698E-02	7.35194E-02	5.79874E-02	3.35858E-02	1.77429E-02	
-0.20000	8.01523E-02	8.29108E-02	8.16526E-02	7.07286E-02	4.66688E-02	2.69450E-02	
-0.10000	7.51772E-02	8.29356E-02	8.56729E-02	8.26216E-02	6.65726E-02	4.61143E-02	
-0.00000	5.93785E-02	7.61085E-02	8.33482E-02	8.76235E-02	8.22105E-02	7.53201E-02	
0.00000		7.61085E-02	8.33482E-02	8.76235E-02	8.22105E-02	7.53201E-02	6.04997E-02
0.10000		4.81348E-02	7.00090E-02	8.63151E-02	8.80624E-02	8.49382E-02	7.76333E-02
0.20000		2.95259E-02	5.13544E-02	7.72739E-02	8.77078E-02	8.84673E-02	8.55909E-02
0.30000		2.07107E-02	3.91681E-02	6.67896E-02	8.29733E-02	8.70779E-02	8.79922E-02
0.40000		1.58301E-02	3.14343E-02	5.81591E-02	7.72710E-02	8.36674E-02	8.74252E-02
0.50000		1.28841E-02	2.64107E-02	5.17403E-02	7.22957E-02	8.01999E-02	8.60001E-02
0.60000		1.10823E-02	2.32170E-02	4.74175E-02	6.88401E-02	7.78121E-02	8.51316E-02
0.70000		1.01614E-02	2.15832E-02	4.53651E-02	6.77032E-02	7.75916E-02	8.61682E-02
0.80000		1.03325E-02	2.19948E-02	4.67328E-02	7.07013E-02	8.16497E-02	9.14855E-02
0.90000		1.31130E-02	2.72721E-02	5.64095E-02	8.41722E-02	9.68476E-02	1.08352E-01
1.00000		4.54878E-02	8.60058E-02	1.53099E-01	2.03657E-01	2.23428E-01	2.39758E-01

Table 1: Replica of Table 8 from Siewert [17]. Plane-parallel Stokes intensities for slab of optical thickness 1.0, single scatter albedo 0.973527, Lambertian albedo 0.0, solar zenith cosine 0.6, for Greek constants Table 1 of Siewert [17].

versus pseudo-spherical, etc.). This battery of tests was completed successfully, but of course it does not validate the complex variable solution (scalar RT has no complex solutions) which is a peculiarity of the vector RTE.

For testing vector formalism, we used the benchmark results noted in [17]; in particular we have reproduced Tables 2-9 in this work. The slab problem used a solar angle 53.130° ($\mu_0 = 0.6$), with single scatter albedo $\omega = 0.973527$, surface albedo 0.0, total layer optical thickness of 1.0, and a set of Greek constants as noted in Table 1 of [17]. Output was specified at a number of optical thickness values from 0 to 1, and at a number of output streams. We chose 24 discrete ordinate streams in the half space for the computation. In Table 1 above, we present our own results for intensity at relative azimuth angle of 180°; the format is deliberately chosen to mimic that in [17]. It is clear that the agreement with Table 8 in [17] is nigh perfect. The only point of issue is the downwelling output at $\mu = 0.6$ which is a limiting case because $\mu_0 = 0.6$; such a case requires l'Hopital's rule to avoid singularity, and this has been implemented in VLIDORT (as in LIDORT), but was not discussed in [17]. All tables in [17] were reproduced, with differences of 1-2 in the sixth decimal place (with the exception of the above limiting case).

A second validation was carried out against the Rayleigh atmosphere results published in the tables of Coulson, Dave and Sekera [19]. These tables apply to a single-layer pure Rayleigh slab in plane parallel geometry; the single scattering albedo is 1.0 and there is no depolarization considered in the scattering matrix. Under these conditions the only surviving Greek constants are: $\beta_0 = 1.0$, $\beta_2 = 0.5$, $\alpha_2 = 3.0$, $\gamma_2 = -\sqrt{6}/2$, $\delta_1 = 1.5$. Tables for Stokes parameters I, Q and U are given for three surface albedos (0.0, 0.25, 0.80), a range of optical thickness values from 0.01 to 1.0, for 7 azimuths from 0ą to 180° at 30° intervals, some 16 view zenith angles with cosines from 0.1 to 1.0, and for 10 solar angles with cosines from 0.1 to 1.0. With the single scattering albedo set to 0.999999, VLIDORT was able to reproduce all these results to within the levels of accuracy specified in the introduction section of the CDS tables. [Greek matrix inputs for Rayleigh scattering with depolarization have been derived for VLIDORT].

5 Initial results for real atmospheres

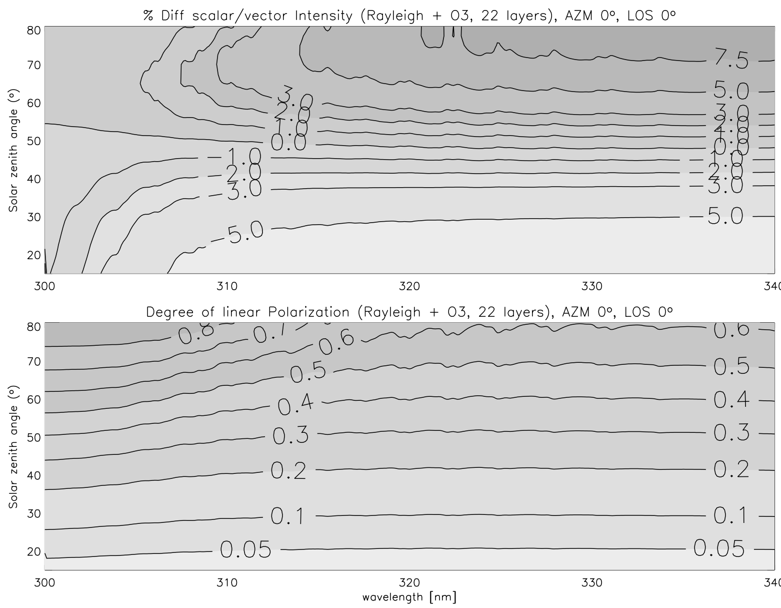

Figure 1: Comparison between full-Stokes intensity and scalar intensity, for nadir viewing (upper panel); corresponding degree of linear polarization (lower panel). Results for a 22-layer Rayleigh atmosphere with ozone absorption. Solar zenith angles and wavelength values as indicated.

In this section we present some results for a real 22-layer atmosphere. We look at wavelengths from 300 to 340 nm for a Rayleigh atmosphere with ozone absorption. Optical thickness values for trace gas absorption and Rayleigh scattering were provided from set-ups used at SAO for the ozone profile retrieval from GOME data (X. Liu, private communication). The depolarization ratios were taken from the latest formulae from Bodhaine et al. [20]. In this case the Greek constants are $\beta_0 = 1.0$, $\beta_2 = \eta$, $\alpha_2 = 6\eta$, $\gamma_2 = -\sqrt{6}\eta$, $\delta_1 = 3\eta$, where $\eta = (1-\rho)/(2+\rho)$ in terms of the depolarization ratio ρ.

Figure 1 shows a complete calculation for one azimuth angle (the principal plane) for the whole wavelength range from 300 to 340 nm, for a complete set of solar zenith angles from 15 to 80 degrees. The top panel shows the difference between vector and scalar computations of the total intensity, expressed as a percentage of the vector intensity. The lower panel show the degree of linear polarization $P = \sqrt{Q^2 + U^2}/I$ (there is no circular polarization in the Rayleigh case). Of interest here is the fact that values of P settle down to their single scattering values as the wavelength falls towards 300 nm - a regime where single scattering increasingly predominates.

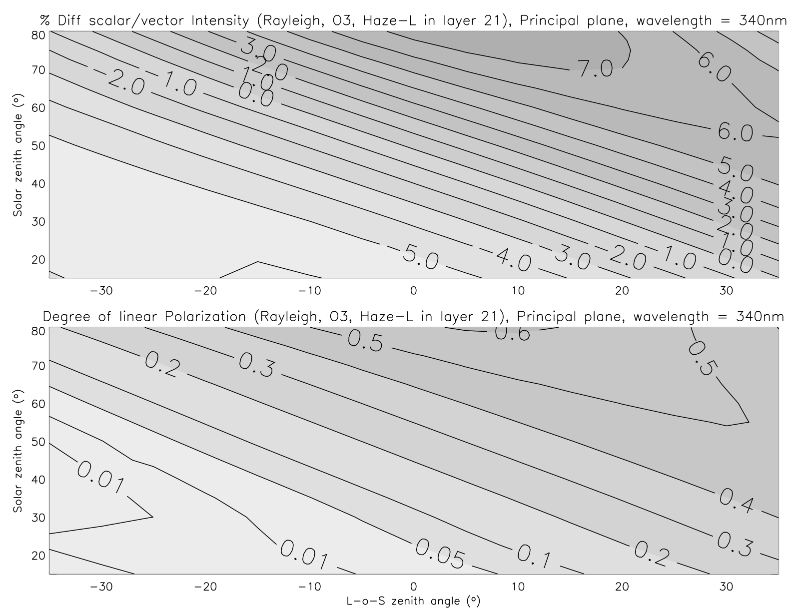

Figure 2: Comparison between full-Stokes intensity and scalar intensity, for nadir viewing (upper panel); corresponding degree of linear polarization (lower panel). Results for a 22-layer Rayleigh atmosphere with ozone absorption, with HAZE-L aerosol in layer 21. Wavelength 340 nm, solar zenith angles and viewing directions in the principal plane as indicated.

A second set of results is presented for the same atmosphere, but this time including aerosol in the penultimate layer close to the ground (between 256 and 512 mb). The aerosol layer has total optical thickness 1.0, and the other optical properties were derived from the Meerhoff Mie program (J. de Haan, private communication). The latter is based on the work of de Rooij and van der Stap [13], and will deliver single scatter albedos and complete sets of Greek constants for any wavelength and for a wide choice of poly-disperse aerosol models. This example (Figure 2) is for the HAZE-L model (modified gamma distribution). The depolarizing effect of aerosol is clear, when we compare the results at 340 nm to those for a Rayleigh atmosphere (Figure

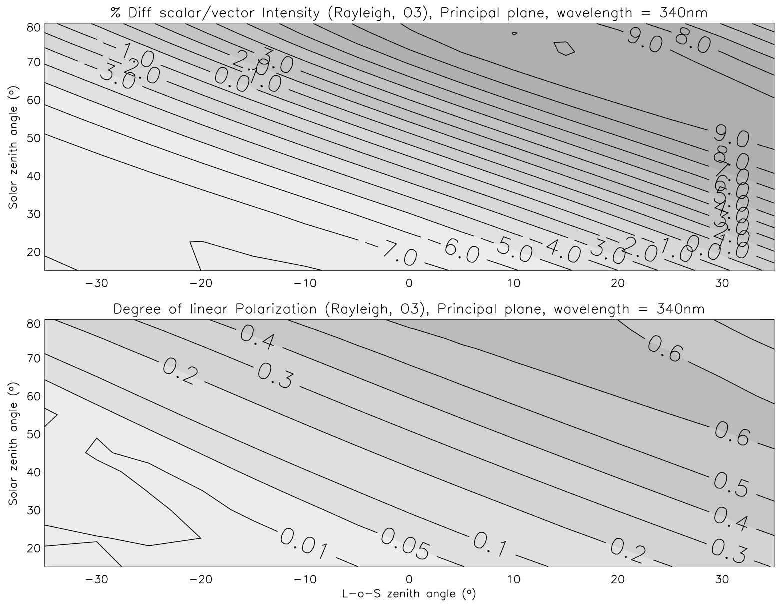

Figure 3: The same as Figure 2, but without the aerosols.

3). Results are shown for a number of solar zenith angles and a range of viewing directions in the principal plane. These calculations were done with 24 discrete ordinate streams in the half space - enough to ensure full accuracy with this kind of aerosol.

6 Concluding Remarks and Future Work

We have reported on the successful implementation of a vector discrete ordinate radiative transfer code VLIDORT that has all the capabilities found in the scalar LIDORT version V2.3, plus an additional option for multi-solar angle processing in one call. We have summarized the first version of this model, and reported benchmark validation tests and initial results. The model will be given its first release in October 2004, concomitant with this Final Report and the completion of User's Guide.

The 2004 VS work was completed with a visit to FMI at the end of September for the implementation of VLIDORT in the surface UV algorithm. This was done as scheduled, and the necessary environment installed for this application of VLIDORT. During the discussions, it became clear that a number of performance enhancements would be very useful to make the program run faster. The most important is the development of a single scatter routine that would give the model the same "approximately-spherical" capacity as LIDORT V2.2+. Methodology for a series of other speed enhancements was worked out, and these improvements would be carried out as part of the second phase of the VLIDORT work.

The other big task for the second phase of VLIDORT is the development of a linearization facility for the generation of analytic weighting functions of the Stokes vector quantities with respect to profile and column elements in the atmosphere, and surface parameters.

A proposal for the second phase of VLIDORT development has been made for 2005, and once this work is done, the VLIDORT model will be ready for all O3 SAF users concerned with polarization issues, and it will have all the capabilities of the scalar model.

7 References

[1] Spurr, R.J.D., T.P. Kurosu, and K.V. Chance, A linearized discrete ordinate radiative transfer model for atmospheric remote sensing retrieval, *JQSRT*, **68**, 689-735, 2001.

[2] Spurr, R.J.D., Simultaneous derivation of intensities and weighting functions in a general pseudo-spherical discrete ordinate radiative transfer treatment, *JQSRT*, **75**, 129-175, 2002.

[3] Van Oss, R.F, and R.J.D. Spurr, Fast and accurate 4 and 6 stream linearized discrete ordinate radiative transfer models for ozone profi le retrieval, *JQSRT*, **75**, 177-220, 2002.

[4] Spurr, R.J.D., A New Approach to the Retrieval of Surface Properties from Earthshine Measurements, *JQSRT*, **83**, 15-46, 2003.

[5] Spurr, R.J.D., LIDORT V2PLUS: a comprehensive radiative transfer package for UV/VIS/NIR nadir remote sensing; a General Quasi-Analytic Solution, *Proc. S.P.I.E. International Symposium, Remote Sensing 2003*, Barcelona, Spain, September 2003.

[6] Chandrasekhar, S., Radiative Transfer, Dover Publications Inc.,New York, 1960.

[7] Siewert, C.E., On the equation of transfer relevant to the scattering of polarized light, *Astrophysics. J.*, **245**, 1080-1086, 1981.

[8] Siewert, C.E., On the phase matrix basic to the scattering of polarized light, *Astron. Astrophys.*, **109**, 195-200, 1982.

[9] Vestrucci, P., and C.E. Siewert, A numerical evaluation of an analytical representation of the components in a Fourier decomposition of the phase matrix for the scattering of polarized light, *JQSRT*, **31**, 177-183, 1984.

[10] Garcia, R.D.M., and C.E. Siewert, A Generalized Spherical Harmonics Solution for Radiative Transfer Models that Include Polarization Effects, *JQSRT*, **36**, 401-423, 1986.

[11] Garcia, R.D.M., and C.E. Siewert, The F_N Method for Radiative Transfer Models that Include Polarization Effects, *JQSRT*, **41**, 117-145, 1989.

[12] Hovenier, J.W., and C.V.M. van der Mee, Fundamental relationships relevant to the transfer of polarized light in a scattering atmosphere, *Astron. Astrophys.*, **128**, 1-16, 1983.

[13] de Rooij, W.A., and C.C.A.H. van der Stap, Expansion of Mie scattering matrices in generalized spherical functions, *Astron. Astrophys.*, **131**, 237-248, 1984.

[14] de Haan, J.F., P.B. Bosma and J.W. Hovenier, The adding method for multiple scattering of polarized light, *Astron. Astrophys.*, **183**, 371-391, 1987.

[15] Stammes, P., J.F. de Haan and J.W. Hovenier, The polarized internal radiation field of a planetary atmosphere, *Astron. Astrophys.*, **225**, 239–259, 1989.

[16] Siewert, C.E., A concise and accurate solution to Chandrasekhar's basic problem in radiative transfer, *JQSRT*, **64**, 109-130, 2000.

[17] Siewert, C.E., A discrete-ordinates solution for radiative-transfer models that include polarization effects, *JQSRT*, **64**, 227-254, 2000.

[18] Wauben, W.M.F., and J.W. Hovenier, *JQSRT*, **47**, 491-500, 1992.

[19] Coulson, K., J. Dave and D. Sekera, Tables related to radiation emerging from a planetary atmosphere with Rayleigh scattering, *University of California Press*, Berkeley, 1960.

[20] Bodhaine,B.A., N.B. Wood, E.G. Dutton and J.R. Slusser, On Rayleigh Optical Depth Calculations, *J. Atmos. Ocean. Tech.*, **16**, 1854-1861, 1999.